

Supernova Remnant 1987A: The Latest Report from the Chandra X-Ray Observatory

Sangwook Park^a Svetozar A. Zhekov^{b,c} David N. Burrows^a
Gordon P. Garmire^a Dick McCray^c

^a*Department of Astronomy & Astrophysics, 525 Davey Lab., The Pennsylvania State University, University Park, PA. 16802, USA*

^b*Space Research Institute, Moskovska str. 6, Sofia-1000, Bulgaria*

^c*JILA, University of Colorado, Box 440, Boulder, CO. 80309, USA*

Abstract

We continue monitoring supernova remnant (SNR) 1987A with the *Chandra X-ray Observatory*. As of 2004 January, bright X-ray spots in the northwest and the southwest are now evident in addition to the bright eastern ring. The overall X-ray spectrum, Since 2002 December, can be described by a planar shock with an electron temperature of ~ 2.1 keV. The soft X-ray flux is now 8×10^{-13} ergs cm^{-2} s^{-1} , which is about five times higher than four years ago. This flux increase rate is consistent with our prediction based on an exponential density distribution along the radius of the SNR between the HII region and the inner ring. We still have no direct evidence of a central point source, and place an upper limit of $L_X = 1.3 \times 10^{34}$ ergs s^{-1} on the 3–10 keV band X-ray luminosity.

Key words: supernovae; general, supernovae; individual (SN 1987A), supernova remnants, X-rays; general

PACS:

1 Introduction

We present the latest results from the *Chandra* observations of supernova remnant (SNR) 1987A. As of 2004 January, we have performed a total of nine observations of SNR 1987A with the Advanced CCD Imaging Spectrometer (ACIS) on board *Chandra* (Table 1). We have presented the results from

Email address: park@astro.psu.edu (Sangwook Park).

the first seven observations in the literature (Burrows et al., 2000; Park et al., 2002; Michael et al., 2002; Park et al., 2004). Previous *Chandra*/ACIS observations of SNR 1987A have revealed a ring-like X-ray morphology with an asymmetric X-ray intensity distribution between the eastern and the western sides of the SNR. X-ray-bright spots have developed around the ring, and soft X-ray flux has been nonlinearly increasing. The X-ray spectrum was found to be thermal in origin, arising from the interaction of the blast wave shock with the circumstellar material. Previous works (Park et al., 2002, 2004) successfully demonstrated that these X-ray features, when compared with the optical and radio emission features, were consistent with the standard physical model: i.e., the SN blast wave shock is approaching the dense inner ring which was produced by non-spherically symmetric stellar winds from the massive progenitor (Michael et al., 2000). In this model, the optically bright spots and the soft X-ray spots are produced by the decelerated shock entering the dense protrusions on the surface of the inner ring, while the radio and the hard X-ray emission features originate from the fast shock propagating into the tenuous HII region between the dense protrusions (Park et al., 2002). Considering its core-collapse, Type II SN origin from a massive progenitor (Sonneborn, Altner, & Kirshner, 1987), as *confirmed* by the detection of the accompanying neutrino burst (Koshiba et al., 1987), the presence of a compact stellar remnant is predicted for SNR 1987A. There has, however, been no evidence for a pointlike source at the center of the remnant, which has been attributed to optically thick stellar ejecta material surrounding the putative central point source (Burrows et al., 2000; Park et al., 2002, 2004).

Table 1. *Chandra* Observations of SNR 1987A

ObsID	Date (Age ^a)	Instrument	Exposure (ks)	Source Counts
124+1387 ^b	1999-10-06 (4609)	ACIS-S + HETG	116	690
122	2000-01-17 (4711)	ACIS-S3	9	607
1967	2000-12-07 (5038)	ACIS-S3	99	9031
1044	2001-04-25 (5176)	ACIS-S3	18	1800
2831	2001-12-12 (5407)	ACIS-S3	49	6226
2832	2002-05-15 (5561)	ACIS-S3	44	6429
3829	2002-12-31 (5791)	ACIS-S3	49	9274
3830	2003-7-8 (5980)	ACIS-S3	45	9668
4614	2004-1-2 (6157)	ACIS-S3	47	11856

^aDay since the SN explosion.

^bThe first observation was split into two sequences.

As the blast wave eventually sweeps through the main body of the dense in-

ner ring, a dramatic increase of the X-ray flux and morphological/spectral changes of SNR 1987A are expected. We continue X-ray observations of SNR 1987A with the *Chandra*/ACIS in order to monitor the dynamic evolution, as well as to discover the central point source, of SNR 1987A. As a continuation of the previous works, we here briefly update the morphological and spectral evolutions of the X-ray remnant of SNR 1987A with two new *Chandra* observations.

2 X-Ray Images

Fig 1 displays the 0.3–8 keV band images of SNR 1987A from the *Chandra*/ACIS observations. SNR 1987A has been significantly brightening for the last \sim four years. As the blast wave enters the main body of the dense inner ring, X-ray-bright spots first appeared on the eastern side of the remnant but have now been developing in the west. SNR 1987A has thus become closer to a *complete* ring than ever.

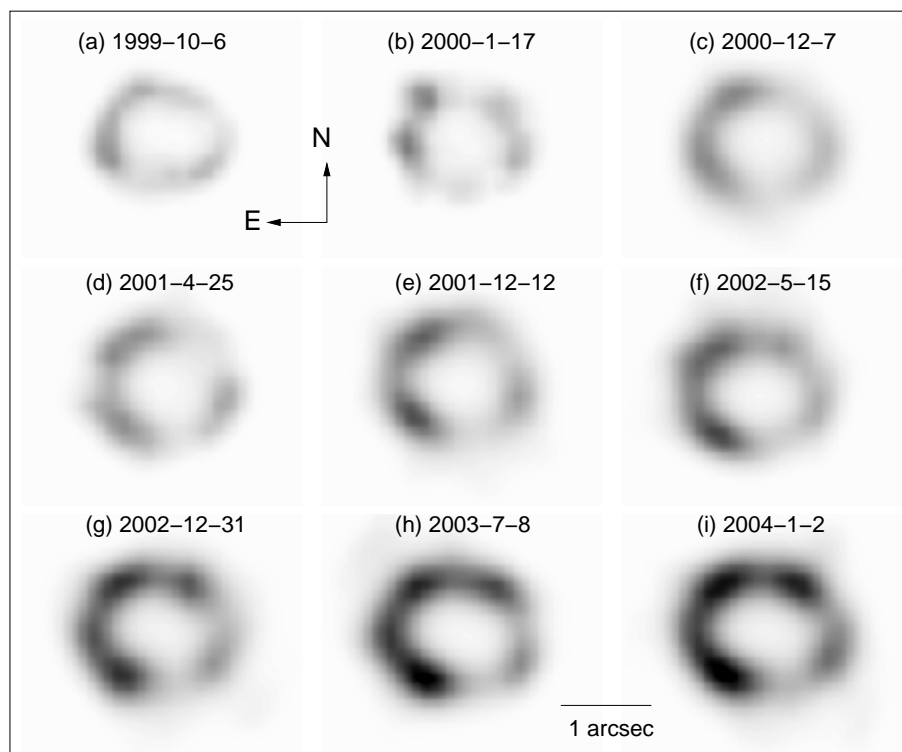


Fig. 1. Exposure-corrected, broadband (0.3–8 keV) X-ray images of SNR 1987A from the *Chandra*/ACIS observations. Images have been deconvolved with the ACIS PSF and then smoothed following the method described in literature (Burrows et al., 2000; Park et al., 2002). Darker gray-scales are higher intensities.

3 X-Ray Spectrum

We perform spectral analysis of SNR 1987A following the procedure presented in Park et al. (2004). The X-ray spectrum can be fitted with a single temperature plane-parallel shock model (Borkowski, Lyerly, & Reynolds, 2001). The fitted foreground column and the elemental abundances are consistent within statistical uncertainties among the individual spectra. It is also reasonably expected that the foreground column and the elemental abundances would not significantly change over a few year-period. We thus fit the observed spectra simultaneously, assuming constant N_H and abundances for the last four years, in order to provide the best constraints on the fitted column and elemental abundances (Fig 2). We varied elemental abundances for N, O, Ne, Mg, Si, S, and Fe, while held in common for all individual spectra. We fixed the abundances for He and C at values appropriate for the ring abundances (Lundqvist & Fransson, 1996), and fixed Ca, Ar, and Ni abundances at the values for the Large Magellanic Cloud (Russell & Dopita, 1992), because the contribution of X-ray line emission from these elemental species in the fitted energy band (0.4 – 5 keV) is insignificant. We varied electron temperature and the ionization timescale freely for individual spectra in order to trace any significant variations in these parameters, as perhaps expected from the shock evolution of this young SNR. For this purpose, we use six spectra with good photon statistics (>6000 counts) for statistically reliable spectral fits. The best-fit parameters (with 2σ uncertainties) are presented in Table 2 and Table 3.

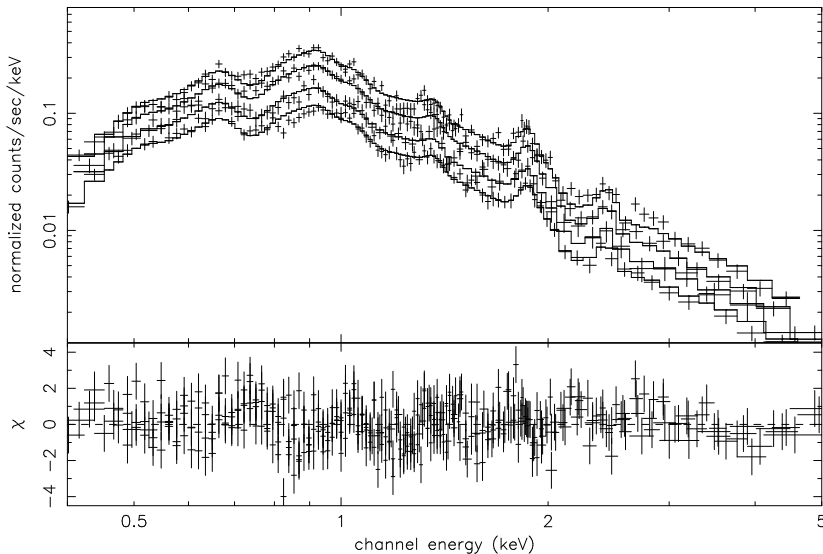


Fig. 2. Four ACIS spectra of SNR 1987A taken between 2000 December (the lowest flux) and 2004 January (the highest flux), separated by \sim one year from each other. The best-fit single-temperature plane-parallel shock model is overlaid with each spectrum.

Until 2002 December, the electron temperature of SNR 1987A has been decreasing while the volume emission measure (EM) was increasing (Park et al., 2004). The latest two observations, however, suggest that the temperature appears to be *constant* since 2002 December, while the EM was continuously increasing (Fig 3). Implications of this recent trend of the electron temperature variation are not straightforward. Park et al. (2004) attributed the decrease of electron temperature to a physical picture where parts of the shock front enter the dense protrusions as the blast wave approaches the inner ring. The latest ACIS images, as well as the HST images, indicate that the blast wave shock front is now entering the dense circumstellar medium (CSM) *all around* the inner ring. The simple physical picture with small portions of the shock front decelerating as it approaches the dense protrusions, then, might not be adequate any longer to describe the overall X-ray spectrum. The X-ray emission might now be dominated by the shock entering the main body of the inner ring. The evolution of the overall electron temperature in this “new phase” of the shock is unclear. For instance, it may continue to soften, but not necessarily in the previously-reported rate, or it may establish a *stable* phase. The details of the shock evolution may be complex depending on thermal conditions of the plasma (e.g., ionization states and/or electron-ion equilibration behind the shock) primarily due to the radial and azimuthal density distribution of the inner ring and its environments. We will need upcoming *Chandra* observations in order to determine whether the latest temperature variation means a truly stable phase or only a temporary state in the course of further, continuous softening of the overall X-ray spectrum.

Table 2. Best-Fit^a Elemental Abundances

Element	Abundance ^b	Element	Abundance ^b	Element	Abundance ^b
He	2.57 (fixed ^c)	Ne	0.20 ^{+0.02} _{-0.04}	Ca	0.34 (fixed ^d)
C	0.09 (fixed ^c)	Mg	0.14 ^{+0.03} _{-0.02}	Ar	0.54 (fixed ^d)
N	0.37 ^{+0.10} _{-0.08}	Si	0.32 ^{+0.05} _{-0.05}	Fe	0.15 ^{+0.01} _{-0.01}
O	0.09 ^{+0.01} _{-0.01}	S	0.84 ^{+0.19} _{-0.18}	Ni	0.62 (fixed ^d)

^a The best-fit $N_H = 1.8^{+0.1}_{-0.2} \times 10^{21} \text{ cm}^{-2}$. $\chi^2/\nu = 699.7/569$.

^b Abundances with respect to solar.

^c Lundqvist & Fransson 1996

^d Russell & Dopita 1992

Although the overall X-ray spectrum of SNR 1987A can be described by a single temperature plane-shock in non-equilibrium ionization (NEI), the physical model of the shock-inner ring interaction indicates that X-ray emission most likely originates from multiple velocity components of the shock in various ionization states. Considering such a multi-component shock, a two-temperature shock model was implemented in order to fit the observed X-ray spectrum

Table 3. Best-Fit Shock Parameters from A Single-Temperature Model^{a,b}.

Date	Electron Temperature (keV)	Ionization Timescale ($10^{10} \text{ cm}^{-3} \text{ s}$)	Emission Measure (10^{57} cm^{-3})
2000-12-7	$2.64^{+0.19}_{-0.20}$	$3.02^{+0.50}_{-0.43}$	$6.84^{+0.36}_{-0.27}$
2001-12-12	$2.48^{+0.35}_{-0.32}$	$2.82^{+0.57}_{-0.43}$	$10.20^{+0.63}_{-0.48}$
2002-5-15	$2.24^{+0.29}_{-0.28}$	$3.23^{+0.65}_{-0.52}$	$12.33^{+0.78}_{-0.66}$
2002-12-31	$2.08^{+0.15}_{-0.14}$	$3.20^{+0.48}_{-0.41}$	$16.68^{+0.93}_{-0.75}$
2003-7-8	$2.11^{+0.14}_{-0.13}$	$3.19^{+0.42}_{-0.38}$	$19.14^{+1.05}_{-0.87}$
2004-1-2	$2.13^{+0.13}_{-0.13}$	$3.29^{+0.45}_{-0.37}$	$22.89^{+1.23}_{-0.96}$

^a $\chi^2/\nu = 699.7/569$.

^b The best-fit $N_H = 1.8^{+0.1}_{-0.2} \times 10^{21} \text{ cm}^{-2}$.

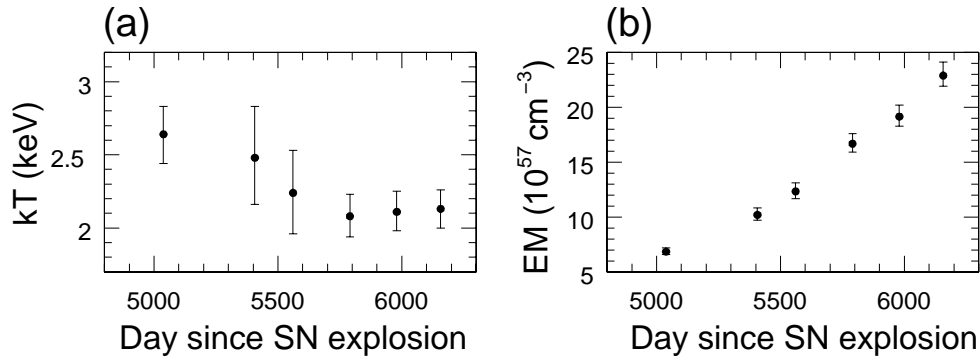


Fig. 3. The electron temperature and EM variations of SNR 1987A.

(Michael et al., 2002; Park et al., 2004). The two-temperature shock model may grossly oversimplify reality, but should be a physically more realistic model than a single shock. In this model, the observed X-ray spectrum originates from two characteristic components. The soft component arises from a slow, decelerated shock entering the dense protrusions of the inner ring. The hard component is produced by a fast shock propagating into the low density HII region. The slow shock was then found to be in collisional ionization equilibrium (CIE), which was reasonable for the shocked dense circumstellar material (Park et al., 2004). Based on these previous results, we apply a two-component model to the latest data (Note: As discussed above, the overall shock phase for the latest X-ray spectrum might be different from that of previous observations. Nonetheless, a two-temperature model should still be a useful approximation for the multi-phase shock). As of 2004 January, an electron temperature of $kT \sim 0.23 \text{ keV}$ is implied for the slow shock in CIE condition, while it is $kT \sim 2.2 \text{ keV}$ for the fast shock in NEI state. The best-fit EMs imply electron densities $n_e \sim 6300 \text{ cm}^{-3}$ for the slow shock and $n_e \sim 280 \text{ cm}^{-3}$ for the fast shock. The hard to soft component EM ratio shows a

noticeable increase since 2002 December (Fig 4), which suggests that a significant increase of the density in the fast shock might have begun. We note that the volume increase of the hard X-ray emitting plasma might also contribute to the observed EM ratio increase. We, however, found that the effect from the volume increase is negligible. This density increase is consistent with the blast wave, for the most parts, now entering the main body of the dense inner ring.

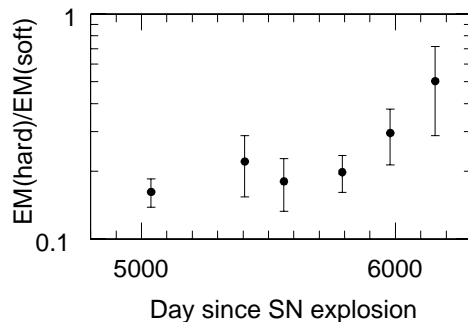


Fig. 4. The hard to soft component EM ratios of SNR 1987A.

4 X-Ray Lightcurve

Fig 5 is the X-ray lightcurve of SNR 1987A. The steep, non-linear increase of the 0.5–2 keV band X-ray flux continues. As of 2004 January, the observed 0.5–2 keV X-ray flux is $f_X \sim 8.2 \times 10^{-13}$ ergs cm⁻² s⁻¹ which is ~ 5 times higher than 1999 October. Following the same method described by Park et al. (2004), we fit the lightcurve assuming an exponential density distribution along the radius of the inner ring. The best-fit model indicates that a density ratio between the high-density inner ring and the low-density HII region (*interior* to the inner ring) is ~ 18 , and that a scale height of the exponential density distribution between inner ring and the HII region is ~ 0.015 pc at a distance of 50 kpc. The estimated density ratio is consistent with the soft to hard component density ratio derived from the two-component spectral fit.

5 Point source

After ~ 17 years of the SN explosion, we still find no direct evidence of a point-like source at the center of SNR 1987A. Utilizing a Monte Carlo simulation (Burrows et al., 2000; Park et al., 2002), we estimate a 90% upper limit on the 3–8 keV band point source counts based on the latest ACIS image of SNR 1987A. We assume a power law spectrum of a photon index $\Gamma = 1.7$ for the putative neutron star in order to estimate the X-ray flux corresponding to the

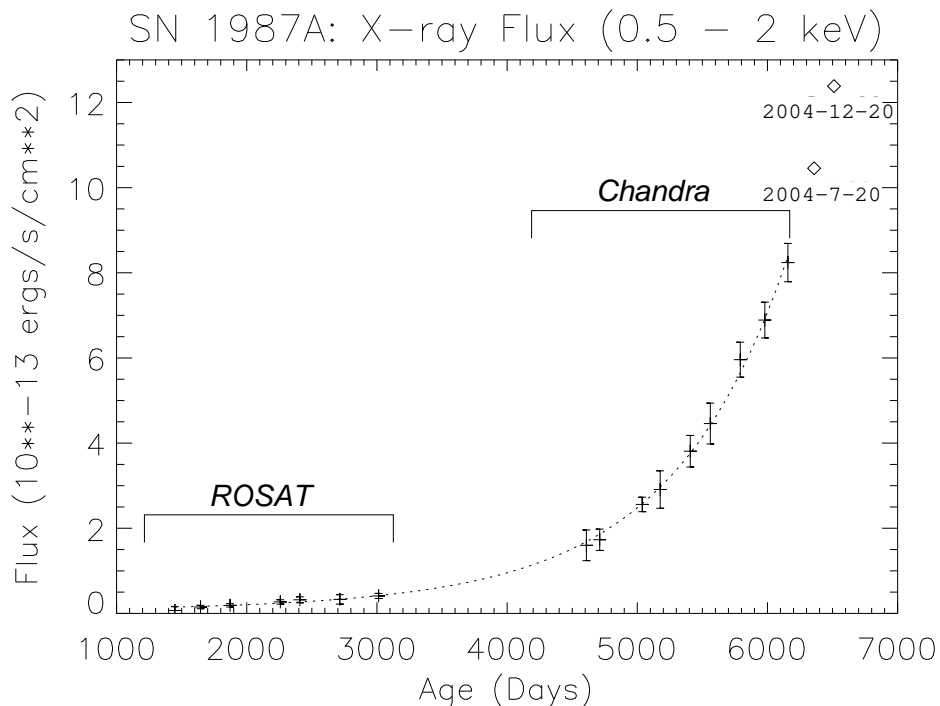


Fig. 5. The X-ray lightcurve of SNR 1987A. The *ROSAT* data points are taken from Hasinger, Aschenbach, & Trümper (1996). The dotted curve is the best-fit model assuming an exponential density profile. Predictions for the next two data points are also marked.

derived upper limit on the point source counts. We note that the absorbing column toward the center of the SNR is highly uncertain depending on the density structure of the actual stellar ejecta prevailing there. Here we assume, as a first-order-estimation, a similar absorbing column N_H as measured from the spectral fitting of the entire SNR. We then obtain an upper limit of $L_X = 1.3 \times 10^{34}$ ergs s⁻¹ on the 3–10 keV band X-ray luminosity of the central point source. Considering higher columns, for instance, if the absorbing column for the point source was an order of magnitude higher than that for the entire SNR, this upper limit could be a few times higher than the above estimate.

References

- Borkowski, K. J., Lyerly, W. J., & Reynolds, S. P. Supernova Remnants In The Sedov Expansion Phase: Thermal X-Ray Emission. *ApJ*, 548, 820–835, 2001
- Burrows, D. N., Michael, E., Hwang, U. et al. The X-Ray Remnant Of SN 1987A. *ApJ*, 543, L149–L152, 2000
- Hasinger, G., Aschenbach, B., & Trümper, J. The X-ray lightcurve of SN 1987A. *A&A*, 312, L9–L12, 1996

- Koshiya, M., Thomas, M., Ryder, S., et al. Supernova 1987A In The Large Magellanic Cloud. IAU Circ. 4338, 1987
- Lundqvist, P. & Fransson, C. The Line Emission From The Circumstellar Gas Around SN 1987A. ApJ, 464, 924–942, 1996
- Michael, E., McCray, R., Pun, C. S. J. et al. Hubble Space Telescope Spectroscopy Of Spot 1 On The Circumstellar Ring Of SN 1987A. ApJ, 542, L53–L56, 2000
- Michael, E., Zhekov, S., McCray, R. et al. The X-Ray Spectrum Of Supernova Remnant 1987A. ApJ, 574, 166–178, 2002
- Park, S., Burrows, D. N., Garmire, G. P. et al. Monitoring The Evolution Of The X-Ray Remnant Of SN 1987A. ApJ, 567, 314–322, 2002
- Park, S., Zhekov, S. A., Burrows, D. N. et al. A Chandra View Of The Morphological And Spectral Evolution Of Supernova Remnant 1987A. ApJ, 610, 275–284, 2004
- Russell, S. C. & Dopita, M. A. Abundances Of The Heavy Elements In The Magellanic Clouds. III - Interpretation Of Results. ApJ, 384, 508–522, 1992
- Sonneborn, G., Altner, B., & Kirshner, R. P. The Progenitor Of SN 1987A - Spatially Resolved Ultraviolet Spectroscopy Of The Supernova Field. ApJ, 323, L35–L39, 1987